

## Interaction of anesthetic supplement thiopental with human serum albumin

Shahper N. Khan<sup>1</sup>, Barira Islam<sup>1</sup>, M. R. Rajeswari<sup>2</sup>, Hammad Usmani<sup>3</sup>,  
and Asad U. Khan<sup>1</sup>✉

<sup>1</sup>Interdisciplinary Biotechnology Unit, Aligarh Muslim University, Aligarh, India; <sup>2</sup>Department of Biochemistry, All India Institute of Medical Sciences, New Delhi, India; <sup>3</sup>Department of Anesthesiology, JN Medical College, AMU, Aligarh, India

Received: 18 August, 2007; revised: 15 January, 2008; accepted: 31 January, 2008  
available on-line: 01 February, 2008

Thiopental (TPL) is a commonly used barbiturate anesthetic. Its binding with human serum albumin (HSA) was studied to explore the anesthetic-induced protein dysfunction. The basic binding interaction was studied by UV-absorption and fluorescence spectroscopy. An increase in the binding affinity ( $K$ ) and in the number of binding sites ( $n$ ) with the increasing albumin concentration was observed. The interaction was conformation-dependent and the highest for the F isomer of HSA, which implicates its slow elimination. The mode of binding was characterized using various thermodynamic parameters. Domain II of HSA was found to possess a high affinity binding site for TPL. The effect of micro-metal ions on the binding affinity was also investigated. The molecular distance,  $r$ , between donor (HSA) and acceptor (TPL) was estimated by fluorescence resonance energy transfer (FRET). Correlation between the stability of the TPL-N and TPL-F complexes and drug distribution is discussed. The structural changes in the protein investigated by circular dichroism (CD) and Fourier transform infrared (FT-IR) spectroscopy reflect perturbation of the albumin molecule and provide an explanation for the heterogeneity of action of this anesthetic.

**Keywords:** thiopental, fluorescence resonance energy transfer, thermodynamics, FT-IR, circular dichroism

### INTRODUCTION

Anesthetic agents have been administered to humans for more than 150 years to provide anesthesia for surgical operations, but their influence on biochemical or physiological processes and the molecular nature of the interactions underlying the functional effect are still poorly understood. Thiopental (TPL), an intravenous barbiturate anesthetic (Fig. 1), is used frequently by anesthesiologists prior to surgery and other invasive medical procedures. In addition to its pharmacological action spectra, TPL is known to exhibit varied effects, e.g. it increases pulmonary inflammation (Giraud *et al.*, 1998), affects bilegenic functions of liver (Skarlosh, 1974), causes

drowsiness in the newborn baby as the drug passes into breast milk; its increased toxicity with higher dose administration has also been reviewed (Krier *et al.*, 1984; Schalen *et al.*, 1992). Human serum albumin (HSA, 66.5 kDa) is the most abundant protein in the blood serum with a concentration of about 0.63 mM. It is a single polypeptide chain of 585 amino acids (Dugiaczyk *et al.*, 1982) with a largely helical ( $\approx 57\%$ ) triple-domain structure that assembles to form a heart-shaped molecule. Other mammalian albumins are highly homologous with human albumin, all of which contain 17 disulfide bridges. HSA considerably contributes to colloid osmotic blood pressure and participates in the transport and distribution of many molecules and metabolites (Peters, 1996). It

✉Corresponding author: Asad U. Khan, Interdisciplinary Biotechnology Unit, Aligarh Muslim University, Aligarh 202002, India; phone: 0091-571-2723088; fax: 0091-571-2721776; e-mail: huzzi99@hotmail.com

**Abbreviations:** ATR, attenuated total reflection; CD, circular dichroism; ext. excitation; FRET, fluorescence resonance energy transfer; FT-IR, Fourier transform infrared spectroscopy; HSA, human serum albumin; MRE, mean residual ellipticity; TPL, thiopental.

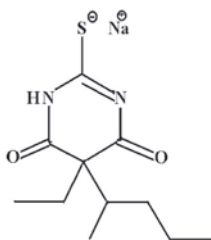


**Figure 1.** Chemical structure of thiopental, a barbiturate anesthetic.

has been shown that the distribution, free concentration and the metabolism of various drugs can be significantly altered as a result of their binding to HSA (Kragh-Hansen, 1981). In studying the interaction of drugs and proteins, fluorescence techniques are commonly used because of their high sensitivity, rapidity and ease of implementation. FT-IR, a powerful technique for the study of hydrogen bonding, has recently become very popular for structural characterization of proteins. For secondary-structure analysis of protein, circular dichroism (CD) spectroscopy is a technique used most frequently. Several reports have been published studying the interaction of proteins with drugs by fluorescence technique (Tian *et al.*, 2003; Sereikaite *et al.*, 2006; Khan *et al.*, 2007), FT-IR (Neault *et al.*, 1998) and CD spectroscopy (Chamouard *et al.*, 1985) but no such data characterizing the mechanism of binding HSA with TPL and the accompanied structural alteration is available. The above methods have advantages over conventional approaches such as affinity and size exclusion chromatography, equilibrium dialysis, ultrafiltration and ultracentrifugation, which suffer from a lack of sensitivity, long analysis time, or both, and use protein concentrations far in excess of the dissociation constant for the drug-protein complex (Epps *et al.*, 1999).

## EXPERIMENTAL

### Materials

Human serum albumin (HSA) of 99% purity was obtained from Sigma Chemical Company (St. Louis, USA). Thiopental (sodium thiopentone) was purchased from Ranbaxy (India). The solutions of TPL and HSA were prepared in 10 mM phosphate buffer of pH 7.4. HSA solutions were prepared based on its relative molecular mass of 66 500. Salts of different metals, phosphate, acetate, glycine and urea were purchased from Merck (India). The protein concentration was determined spectrophotometrically using the absorption coefficient of 36 500  $M^{-1} \text{ cm}^{-1}$  at 280 nm (Painter *et al.*, 1998). All other materials were of analytical reagent grade and double distilled water was used throughout.

### Apparatus

The absorbance spectra were recorded on a double beam Shimadzu UV-Vis spectrophotometer UV-1700 using a cuvette of 1 cm path length. Fluorescence measurements were performed on a spectrofluorimeter Model RF-5301PC (Shimadzu, Japan) equipped with a 150 W Xenon lamp and a slit width of 10 nm. A 1.00 cm quartz cell was used for measurements. The CD measurements were made on a JASCO-J-820 spectropolarimeter (Tokyo, Japan) using a 0.1 cm cell at 0.2 nm intervals, with three scans averaged for each CD spectrum in the range of 200–350 nm. FT-IR measurements were made at room temperature on a Nicolet Nexus 670 FT-IR spectrometer (USA) equipped with a germanium attenuated total reflection (ATR) accessory, a DTGS KBr detector and a KBr beam splitter.

### Procedures

**UV measurements.** The UV measurements of HSA in the presence and absence of TPL were made in the range of 200–300 nm and HSA concentration was fixed at 12  $\mu\text{M}$  while the drug concentration was varied from 12 to 48  $\mu\text{M}$ .

**Drug-protein interactions.** The HSA concentration was fixed at 3  $\mu\text{M}$  unless mentioned otherwise and the drug concentration was varied from 3 to 30  $\mu\text{M}$ . Fluorescence spectra were recorded at three temperatures (298, 308 and 318 K) in the range of 300–400 nm upon excitation at 280 nm. To evaluate the effect of ionic environment on interaction the ionic strength was maintained with NaCl at 100, 200 or 400 mM. In substrate-dependent binding the three protein concentrations taken were 3, 6 and 9  $\mu\text{M}$ .

**Conformation-dependent interaction.** Human serum albumin exists in different conformational states as the N, B, F and I forms (Ahmad *et al.*, 2006). The N, B, F and I conformations were prepared by mixing 20  $\mu\text{l}$  of HSA monomer stock solution (250  $\mu\text{M}$ ) with 980  $\mu\text{l}$  of pH 7 (60 mM phosphate), pH 9 (10 mM glycine/NaOH), pH 3.5 (10 mM acetate) buffers and 10 M urea was added as per the required concentration. The existence of different isomers in the experimental preparations was confirmed basing on the various fluorescence properties of the different forms. The  $\lambda_{\text{max}}$  of the N form = 344 (ext. 295 nm), 339.3 (ext. 280 nm);  $\lambda_{\text{max}}$  of the B form = 340 (ext. 295 nm), 334 (ext. 280 nm);  $\lambda_{\text{max}}$  of the F form = 344 (ext. 295 nm), 334.6 (ext. 280 nm);  $\lambda_{\text{max}}$  of the I form = 344 (ext. 295 nm), 341 (ext. 280 nm) and fluorescence intensity of N, B, F and I forms are 101, 96, 115 and 71, respectively, with excitation and emission slits at 5 and 10 nm.

**Fourier transform infrared (FT-IR) spectroscopy.** All spectra were taken *via* the attenuated total

reflection (ATR) method with resolution of  $4\text{ cm}^{-1}$  and 60 scans. Spectra processing procedure: spectra of buffer and protein solution were collected at the same conditions. Then, buffer spectrum is subtracted from the spectra of sample solution to get the FT-IR spectra of proteins. The subtraction criterion was that the original spectrum of protein solution between  $2200$  and  $1800\text{ cm}^{-1}$  was without any important feature (featureless) (Surewicz *et al.*, 1993).

**Circular dichroism (CD) measurements.** The CD measurements of HSA in the presence and absence of TPL were made in the range of  $200\text{--}300\text{ nm}$  using a  $0.1\text{ cm}$  cell at  $0.2\text{ nm}$  intervals with three scans averaged for each CD spectrum. A  $150\text{ }\mu\text{M}$  stock solution of each form of HSA was prepared in  $10\text{ mM}$  phosphate buffer. The molar ratios of HSA to drug concentration were  $1:10$ ,  $1:11$ ,  $1:12$  and  $1:14$ .

#### Energy transfer between TPL and protein.

The absorbance spectrum of TPL ( $3\text{ }\mu\text{M}$ ) was recorded in the range of  $300\text{--}400\text{ nm}$ . The emission spectrum of HSA ( $3\text{ }\mu\text{M}$ ) was also recorded in the range of  $300\text{--}400\text{ nm}$ . The overlap of the UV absorbance spectrum of TPL with the fluorescence emission spectrum of the protein was used to calculate the energy transfer.

**Effects of some divalent ions.** Fluorescence spectra of TPL-HSA were recorded in the presence and absence of various ions, *viz.*,  $\text{Cu}^{2+}$ ,  $\text{Fe}^{3+}$ ,  $\text{Ni}^{2+}$ ,  $\text{Zn}^{2+}$ ,  $\text{Mn}^{2+}$  and  $\text{Ca}^{2+}$  and in the range of  $300\text{--}400\text{ nm}$  upon excitation at  $280\text{ nm}$ . The concentration of HSA was fixed at  $3\text{ }\mu\text{M}$  and that of the common ion was maintained at  $10\text{ }\mu\text{M}$ .

## RESULTS AND DISCUSSION

### UV-Vis absorbance studies

The interaction between TPL-HSA was studied from the UV-Vis absorbance spectral data (Fig. 2). The UV absorbance intensity of HSA increased with the increasing TPL concentration. The addition of the drug results in a distinct shift of the TPL-HSA spectrum toward longer wavelength (red shift). These results clearly indicated an interaction and some complex formation between TPL and HSA (Hu *et al.*, 2004; Cui *et al.*, 2004).

### Binding of TPL to HSA

Fluorescence measurements can give some information on the binding of small molecules to the protein, such as the binding mechanism, binding mode, binding constants, binding sites and intermolecular distances. Fluorescence intensity of a compound can be decreased by a variety of molecular interactions, *viz.*, excited-state reactions, molecular

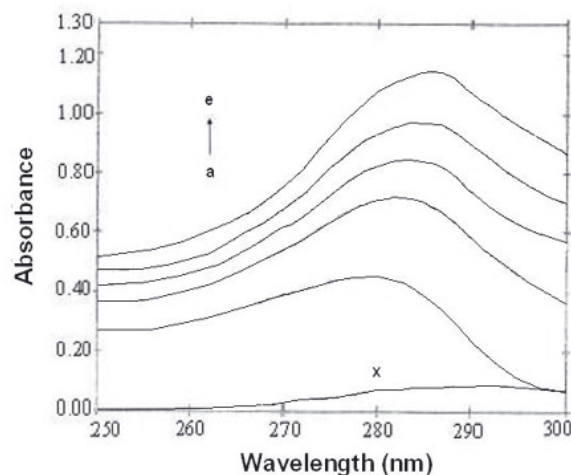


**Figure 2. Absorbance spectra of HSA, TPL and HSA-TPL system.**

HSA concentration was  $12\text{ }\mu\text{M}$  (a). TPL concentration for TPL-HSA system was at  $12\text{ }\mu\text{M}$  (b),  $24\text{ }\mu\text{M}$  (c),  $36\text{ }\mu\text{M}$  (d) and  $48\text{ }\mu\text{M}$  (e). A concentration of  $12\text{ mM}$  TPL (x) was used for TPL only.

rearrangements, energy transfer, ground state complex formation and collisional quenching. Such a decrease in intensity is called quenching. Fluorescence spectra of HSA in the presence of different amounts of TPL were recorded in the range of  $300\text{--}400\text{ nm}$  upon excitation at  $280\text{ nm}$ . TPL caused a concentration-dependent quenching of the intrinsic fluorescence of HSA (Fig. 3) without changing the emission maximum and shape of the peaks. These results indicated that there were interactions between TPL and HSA and the binding resulted in a non-fluorescent complex. The fluorescence quenching data was analyzed by the Stern-Volmer equation:

$$F_0/F = 1 + K_{SV} [Q] \quad (1)$$

where  $F_0$  and  $F$  are the steady-state fluorescence intensities in the absence and presence of quencher, respectively,  $K_{SV}$  the Stern-Volmer quenching constant and  $[Q]$  is the concentration of quencher (TPL). The values of  $K_{SV}$  and  $R^2$  (regression coefficient) are shown in Table 1. The pattern of the  $F_0/F$  versus  $[Q]$  (Stern-Volmer) plots for HSA (Fig. 4) revealed the quenching type, may be static or dynamic, since the characteristic Stern-Volmer plot of combined quenching (both static and dynamic) is an upward curve (as in the Fig. 4). Stern-Volmer plot, however, does not define *per se* the quenching type in the present study, and an additional information is required for this determination. One way to distinguish dynamic from static quenching is to examine the temperature effect on the interaction of the drug with HSA. The  $K_{SV}$  values decrease with an increase in temperature for static quenching, but the reverse

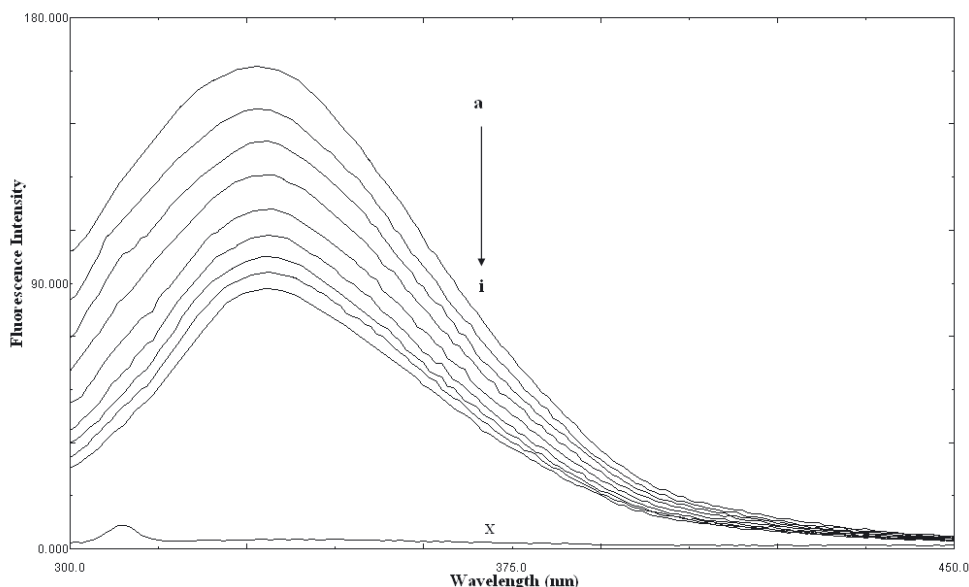


**Figure 3. Fluorescence emission spectra of HSA in the absence and presence of TPL.**

HSA at 3  $\mu\text{M}$  (a) in phosphate buffer, pH 7.4, temperature 298 K in the absence and presence of TPL after excitation at 280 nm. The TPL concentration was 3  $\mu\text{M}$  (b), 6  $\mu\text{M}$  (c), 9  $\mu\text{M}$  (d), 12  $\mu\text{M}$  (e), 15  $\mu\text{M}$  (f), 18  $\mu\text{M}$  (g), 21  $\mu\text{M}$  (h), 24  $\mu\text{M}$  (i) and 3  $\mu\text{M}$  TPL alone (x).

effect will be observed for dynamic quenching. The results of the present study indicate that the probable quenching mechanism of fluorescence of HSA by TPL is static quenching. The mechanism of quenching was further confirmed from the values of quenching rate constants,  $K_q$ , which are evaluated using the equation:

$$K_q = K_{SV} / \tau_0 \quad (2)$$

where  $\tau_0$  is the average lifetime of the protein without the quencher. Various values of fluorescence lifetime for HSA have been reported but the average fluorescence lifetime used was about 5 ns (Gelamo *et al.*, 2002) and hence the values of  $K_q$  were of the order of  $10^{11} \text{ L} \cdot \text{mol}^{-1} \cdot \text{s}^{-1}$  (Table 1), which is greater than the

maximum scatter collision quenching constant  $K_q$  ( $2 \times 10^{10} \text{ L} \cdot \text{mol}^{-1} \cdot \text{s}^{-1}$ ) for various quenchers with a biopolymer. This implies that the quenching is initiated by the formation of a complex (Ware, 1962).

#### Analysis of binding equilibria

When small molecules bind independently to a set of equivalent sites on a macromolecule, the equilibrium between free and bound molecules is given by the equation (Feng *et al.*, 1998; Gao *et al.*, 2004):

$$\log [(F_0 - F)/F] = \log K + n \log [Q] \quad (3)$$

where  $K$  and  $n$  are the binding constant and the number of binding sites, respectively. Thus, the plot of  $\log (F_0 - F)/F$  versus  $\log [Q]$  can be used to determine  $K$  as well as  $n$ . The values of  $K$  were found to be  $(2.52 \pm 0.021) \times 10^3$ ,  $(2.20 \pm 0.042) \times 10^3$  and  $(1.74 \pm 0.056) \times 10^3 \text{ M}^{-1}$  for HSA at 298, 308 and 318 K, respectively. The values of  $n$  were  $(0.86 \pm 0.02)$ ,  $(0.86 \pm 0.06)$  and  $(0.82 \pm 0.04)$ , respectively, at 298, 308 and 318 K. It was found that the binding constant decreased with an increase in temperature, resulting in the destabilization of the TPL-HSA complex. Meanwhile, from the data of  $n$  it may be inferred that there is one independent class of binding sites on HSA for TPL.

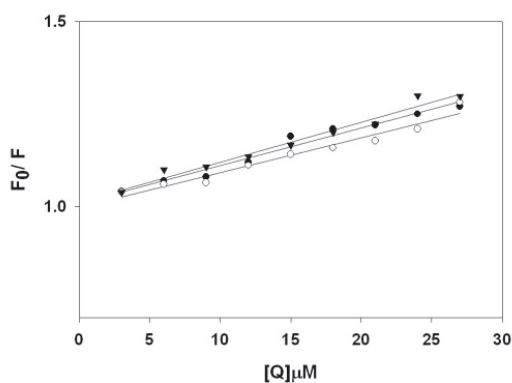


**Figure 4. Stern-Volmer plot for the binding of TPL with HSA.**

Data for: 298 K (●), 308 K (○) and 318 K (▼) are shown.

#### Substrate-dependent binding

It was observed that the binding increased with the increasing concentration of albumin (sub-

Table 1. Thermodynamic parameters of HSA–TPL system

T (K)	$K_{SV} \times 10^3$ (L mol <sup>-1</sup> )	$Kq \times 10^{11}$ (L mol <sup>-1</sup> s <sup>-1</sup> )	$R^2$	$\Delta G^\circ$ (KJ mol <sup>-1</sup> )	$\Delta H^\circ$ (KJ mol <sup>-1</sup> )	$\Delta S^\circ$ (J mol <sup>-1</sup> K <sup>-1</sup> )
298	1.00 ± 0.04	2.000 ± 0.041	0.9675	-19.421 ± 0.007		
308	0.98 ± 0.05	1.960 ± 0.050	0.9580	-19.723 ± 0.004	-14.06 ± 0.04	18.02 ± 0.03
318	0.95 ± 0.02	1.900 ± 0.022	0.9708	-19.730 ± 0.006		

strate) at fixed TPL (ligand) molar ratios. The quenching effect increases with the higher concentration of albumin (Fig. 5), resulting in an increase in the magnitude of binding affinity and binding capacity of this interaction (Table 2). This confirms the strengthening of binding forces governing the reaction. This could be explained by the fact that each albumin molecule represents a large lipophilic or at least hydrophobic area for the lipophilic TPL, which provides a better site for localization of TPL molecules.

Our study suggests that even a single dose of the drug can cause pronounced alteration in physico-chemical properties of bound protein.

### Conformation-dependent binding

The transition of serum albumin from N to B and B to F led to a change in its conformational state. Figure 6 shows pronounced quenching in the F-form compared to other two forms. This difference in fluorescence quenching/TPL binding pattern here could be attributed to a change in protein conformation. This may be due to a close exposure of the drug to its binding site due to unfolding and breakage of interdomain bridges in the protein. Conformation-dependent reduction in binding parameters has also been described previously for warfarin (Wilting *et al.*, 1980).

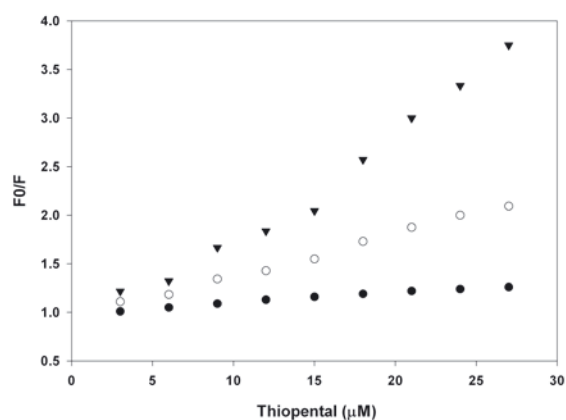


Figure 5. Stern–Volmer plot for the binding of TPL with HSA at different concentrations.

Concentration of HSA were (●) 3 μM, (○) 6 μM, (▼) 9 μM. This shows the magnification of drug interaction of same dose in the presence of higher concentration of albumin.

### Correlation of conformation with drug distribution

Binding in the serum can influence drug distribution in the body and the magnitude of the effect will depend on the strength of  $K_a$  and on the dose of the drug (Ryan *et al.*, 2004). The stability of the complex in acidic conditions is of immense physiological relevance in view of its elimination and excretion. The complex of TPL with the F-conformation of HSA is much stronger than those with the other, N and B, forms as indicated by the association constants (Table 3). The increase in the binding affinities with conformational transition of HSA may strongly affect both the dose-response relationship and the rate of drug elimination (Borga & Borga, 1997 Ryan *et al.*, 2004). The dose response relationship and the rate of drug elimination depend on the fraction of free drug ( $\alpha_f$ ) in the body, and the fraction of total drug present in the free form  $[D_f]$  depends on  $K$  ( $1/K_{dis}$ ) for a given drug concentration according to the following equation (Martin *et al.*, 1965).

$$\alpha_f = (K_{dis} + [D_f]) / ([P_t] + K_{dis} + [D_f]) \quad (4)$$

Where  $[P_t]$  is total protein concentration and  $K_{dis}$  is dissociation constant. A strongly bound drug at low concentration is concentrated mainly in the blood plasma component. There is a dose range within which a small increase in the dose results in a relatively large increase in the amount of unbound drug. When  $[D_f] \rightarrow 0$ ,  $\alpha$  becomes proportional to  $K_{dis}$

$$\alpha_f = K_{dis} / ([P_t] + K_{dis}) \quad (5)$$

At the plasma concentration of HSA ( $6.7 \times 10^{-4}$  M), the fraction of free TPL was calculated according to Eqn. 5 and was found to be about 71% higher for the N isomer as compared to the F isomer.

### pH dependence of $K$ ascribed to conformational changes of HSA

Whether the pH dependence of the binding affinity  $K$  resides in the ionic state of TPL or the protein molecule remains an interesting point. The extent of ionization of TPL (Fig. 1) (NH,  $pK = 8.63$ ) was determined according to Henderson–Hasselbalch:

$$pH = pK + \log [\alpha / (1 - \alpha)] \quad (6)$$

**Table 2. Substrate dependent increase in the binding parameters at constant thiopental concentration**

HSA [ $\mu\text{M}$ ]	$K$ ( $\text{M}^{-1}$ )	$n$	$\Delta G^\circ_{\text{binding}}$ ( $\text{KJ mol}^{-1}$ )
3	$2.5 \times 10^3 \pm 0.26$	$0.86 \pm 0.03$	$-19.421 \pm 0.007$
6	$1.8 \times 10^5 \pm 0.19$	$1.09 \pm 0.06$	$-30.241 \pm 0.004$
9	$8.5 \times 10^6 \pm 0.08$	$1.36 \pm 0.02$	$-39.861 \pm 0.008$

where  $\alpha$  is the extent of protonation and  $pK$  is the extent of ionization. Using this equation, the following equations were derived which describe the extent of ionization of ionizing groups of TPL at pH 3.5, 7 and 9.

pH 3.5  $pH = pK - 5.13$  approx. 100%  $-\text{NH}_2^+$

pH 7.0  $pH = pK - 1.63$  approx. 99%  $-\text{NH}_2^+$

pH 9.0  $pH = pK + 0.37$  approx. 30%  $-\text{NH}_2^+$

Based on these, the ionic state of TPL at different pH values was determined, and it can be noted that TPL has an almost equal positive charge at pH 3.5 and 7.0. The increase in the magnitude of  $K$  at acidic pH and not at neutral pH indicated that the origin of the pH dependence of  $K$  resided mainly in the protein molecule. This could be clearly explained with the help of the conformational differences at these pH.

#### Binding site of TPL on domain II

The acid- and urea-induced unfolding pathway was employed to locate the binding site (Ahmad *et al.*, 2006) for TPL on HSA. HSA undergoes the N $\rightarrow$ F and N $\rightarrow$ I transitions induced by the acidic pH between 7.0–3.5 and the urea concentration in the range of 4.8–5.2 M, respectively (Chmelik & Kalous, 1982; Khan, 1986). The F isomer, which predominates at pH 3.5, is characterized by unfolding and separation of domain III, and isomer I is characterized by unfolding of domain III and partial but significant loss of native conformation of domain I. Domain II is known to be unaffected by either N $\rightarrow$ F or N $\rightarrow$ I transitions. Hence, no effect in the number of binding sites (approx. 0.81) of these conformational states compared to native (Table 3) is suggestive of the location of the binding sites for TPL on domain II. The increase in the binding affinity and

almost the same number of binding capacity in the F form indicates a better availability of the binding site due to unfolding of domain III. The small decrease in the ( $n$ ) value may be due to a loss of inter domain interactions which stabilizes the protein domain structure.

#### Types of interaction force between HSA and TPL

Considering the dependence of the binding constant on temperature, a thermodynamic process was considered to be responsible for this interaction. Therefore, the thermodynamic parameters dependent on temperature were analyzed in order to further characterize the forces acting between TPL and HSA. The forces acting between a small molecule and a macromolecule mainly include hydrogen bonds, van der Waals forces, electrostatic forces and hydrophobic interaction forces. The thermodynamic parameters, enthalpy change ( $\Delta H^\circ$ ), entropy change ( $\Delta S^\circ$ ) and free energy change ( $\Delta G^\circ$ ) are the main evidence to determine the binding mode. The thermodynamic parameters were evaluated using the following equations:

$$\log K = -\frac{\Delta H^\circ}{2.303RT} + \frac{\Delta S^\circ}{2.303R} \quad (7)$$

$$\Delta G^\circ = \Delta H^\circ - T\Delta S^\circ \quad (8)$$

where  $K$  and  $R$  are the binding constant and gas constant, respectively. The results obtained are shown in Table 1. The positive entropy change occurs because the water molecules that are arranged in an orderly fashion around the ligand and protein acquire a more random configuration as a result of hydrophobic interactions. A negative  $\Delta H^\circ$  value is observed whenever there is hydrogen bonding in the binding (Ross & Subramanian, 1981; Rahman *et al.*, 1993). The negative  $\Delta H^\circ$  and positive  $\Delta S^\circ$  values in the case of TPL, therefore, show that both hydrogen bonds and hydrophobic interactions play a role in the binding of TPL to HSA (Aki & Yamamoto, 1989; Seedher *et al.*, 1999). This is in agreement with the insignificant effect due of functional group ionization on binding (charged species).

**Table 3. Comparative assessment of quenching constants and TPL binding parameters to isomeric forms of HSA**

HSA isomers	$K$ ( $\times 10^3 \text{ M}^{-1}$ )	$n$	$\Delta G^\circ_{\text{binding}}$ ( $\text{KJ mol}^{-1}$ )
Native (N)	$2.50 \pm 0.26$	$0.86 \pm 0.03$	$-19.421 \pm 0.007$
Basic (B)	$2.48 \pm 0.11$	$0.90 \pm 0.01$	$-19.307 \pm 0.002$
Fast moving (F)	$5.42 \pm 0.03$	$0.82 \pm 0.06$	$-21.371 \pm 0.003$
Urea induced (I)	$5.29 \pm 0.04$	$0.80 \pm 0.02$	$-21.211 \pm 0.006$

#### Structure-ascribed synchronous fluorescence

Intrinsic fluorescence of HSA was studied to evaluate tertiary structure changes induced as a result of the interaction between TPL and HSA. Synchronous mode of fluorescence spectroscopy in-

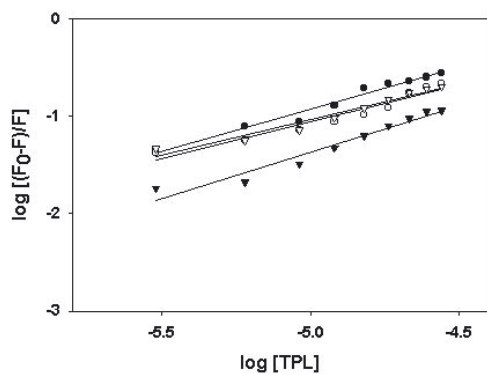


**Figure 6. Conformation dependent binding.**

The plot of  $\log [(F_0-F)/F]$  versus  $\log [Q]$  for (●) N, (○) B, (▼) F and (▽) I conformation of HSA for binding constant and binding sites.

troduced by Lloidy (1971), was applied to infer the conformational changes of the protein due to this binding reaction. Simultaneous scanning of excitation and the emission wavelengths with a fixed wavelength difference between them was done. It gives information about the change in the molecular environment of the protein due to ligand binding. It provides several advantages over other modes like spectral simplification, reduction in spectral noise and spectral area. According to Miller (1979), the characteristic information of tryptophan residue is obtained when  $\Delta\lambda$  difference is maintained at 60 nm. Figure 7 shows that addition of TPL results in strong fluorescence diminution of tryptophan with

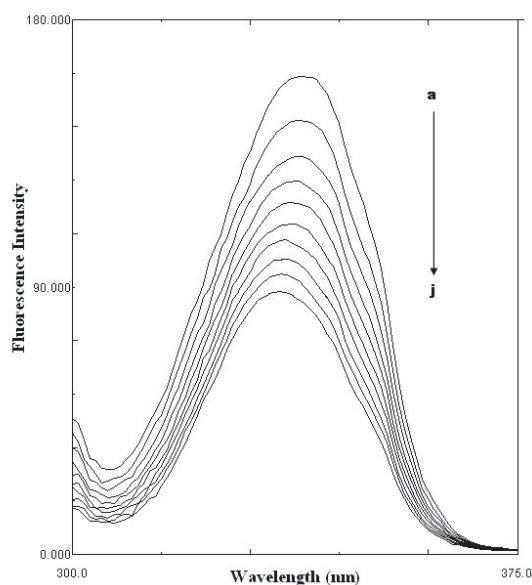


**Figure 7. Synchronous fluorescence spectra of HSA.**

The spectra of HSA (3  $\mu\text{M}$ ) with  $\Delta\lambda = 60$  nm in increasing concentration of TPL: 0  $\mu\text{M}$  (a), 3  $\mu\text{M}$  (b), 6  $\mu\text{M}$  (c), 9  $\mu\text{M}$  (d), 12  $\mu\text{M}$  (e), 15  $\mu\text{M}$  (f), 18  $\mu\text{M}$  (g), 21  $\mu\text{M}$  (h), 24  $\mu\text{M}$  (i) and 27  $\mu\text{M}$  (j).

the maximum emission wavelength at 338–332 nm. As suggested earlier, the maximum emission wavelength ( $\lambda_{\text{max}}$ ) at 330–332 indicated that tryptophan residues are located in a nonpolar region, i.e. they are buried in a hydrophobic pocket in HAS, and  $\lambda_{\text{max}}$  at 350–352 nm shows that tryptophan residues are exposed to water, that is, the hydrophobic cavity in HSA is exposed due to disagglomeration of HSA domains. Figure 7 suggests that TPL mainly bound to the hydrophobic regions of HSA, which is in accordance with the results from the binding mode.

#### FT-IR measurements

Additional evidence regarding the TPL–HSA complexations comes from FT-IR spectroscopy results obtained for drug–protein complexes. Infrared spectra of proteins exhibit a number of so-called amide bands which represent different vibrations of the peptide moiety. Of all the amide modes of the peptide group, the single most widely used one in studies of protein secondary structure is amide I. This vibration mode originates from the C=O stretching vibration of the amide group (coupled to the in-phase bending of the N–H bond and the stretching of the C–N bond) and gives rise to infrared bands in the region between approx. 1600 and 1700  $\text{cm}^{-1}$

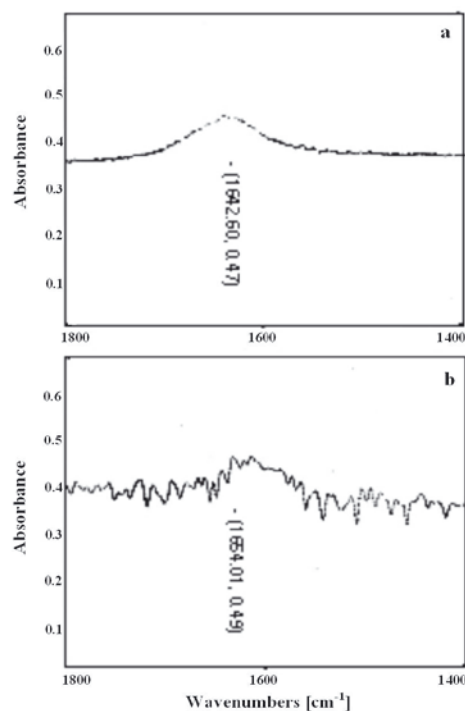


**Figure 8. Fourier transform infrared spectroscopy.**

FT-IR spectra and difference spectra of HSA in aqueous solution (a) FT-IR spectrum of HSA; (b) FT-IR difference spectrum of HSA obtained by subtracting the spectrum of the TPL+ buffer from that of the TPL-bound form in the region of 1800–1400  $\text{cm}^{-1}$  at physiological pH (HSA, 3.0  $\mu\text{M}$ ; TPL, 6.0  $\mu\text{M}$ ).

**Table 4. Alterations in protein secondary structures induced by TPL binding with HSA**

Structure change (%)				
TPL/HSA (molar ratio)	$\alpha$	$\beta$	Turns	Random
0	54.6	23.2	16.2	6.0
10	49.6	18.5	22.5	9.4
11	48.2	17.4	23.1	11.3
12	47.4	16.6	23.8	12.2
14	45.8	15.7	24.6	13.9

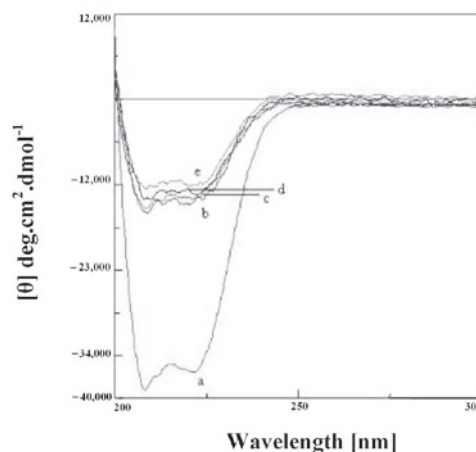
(Surewicz *et al.*, 1993). The protein amide bands have a relationship with the secondary structure of protein, and amide I band is more sensitive to the change of protein secondary structure than amide II (He *et al.*, 2005). Figure 8 shows the FT-IR spectra of free and TPL-bound form of HSA with its difference absorbance spectrum. The spectrum in Fig. 8a was obtained by subtracting the absorbance of phosphate buffer from the spectrum of protein solution. The difference spectrum shown in Fig. 8b was obtained by subtracting the spectrum of TPL+ buffer from that of the TPL-bound HSA. The evident peak shift of amide I band from 1642.60 to 1654.01  $\text{cm}^{-1}$  and the appearance of new peaks in Fig. 8b indicate that the secondary structure of HSA is changed when TPL is added.

#### Circular dichroism studies

In this work, the molar ratios of 1:10, 1:11, 1:12 and 1:14 for HSA/TPL were used to prepare sample for CD measurements. Each sample contained fixed concentration of protein (6  $\mu\text{M}$ ) with varied drug concentration. The CD spectra of HSA in the absence (line a) and presence (lines b to e) of TPL are shown in Fig. 9. The CD spectra of HSA exhibited two negative bands in the UV region at 208 and 220 nm, characteristic of an  $\alpha$ -helical structure of protein (Hu *et al.*, 2005). The CD results were expressed in terms of mean residual ellipticity (MRE) in  $\text{deg} \cdot \text{cm}^2 \cdot \text{dmol}^{-1}$  according to the following equation:

$$[\theta] = \frac{\text{observed CD (mdeg)}}{C_{pnl} \times 10} \quad (9)$$

Where  $[\theta]$  is mean residual ellipticity,  $C_p$  is the molar concentration of the protein,  $n$  the number of amino-acid residues and  $l$  is the path length. The instrument was installed with software based on Yang equation (Chen *et al.*, 1971) to calculate the secondary structure content in the protein. The CD spectrum of native HSA alone showed very neat

**Figure 9. Secondary structure estimation by circular dichroism.**

Far UV-CD spectra of HSA of native, (a); native + 30  $\mu\text{M}$  TPL, (b); native + 33  $\mu\text{M}$  TPL, (c); native + 36  $\mu\text{M}$  TPL, (d); native + 42  $\mu\text{M}$  TPL, (e), respectively.

**Table 5. The binding constants  $K'$  ( $\text{M}^{-1}$ ) between TPL and HSA at 25°C in the presence of divalent ions**

Ions	$K' (\times 10^3)$	$R^2$	$K'/K$
Ca	4.50	0.9755	1.78
Mn	13.00	0.9980	5.15
Zn	2.60	0.9969	1.03
Cu	83.50	0.9825	33.13
Ni	31.50	0.9893	12.50
Fe	9.28	0.9928	1.76

peaks at 208 and 222 nm, which are negative in Fig. 9. Addition of TPL resulted in drastic reduction in ellipticity (curve b), which further reduces on addition of the TPL (Fig. 9; curve c, d and e). The change in ellipticity is accompanied by a decrease in both  $\alpha$ -helix and  $\beta$ -sheet structures (Table 4) illustrating the change in the secondary structure of HSA. It is important to note that saturable binding of some anesthetics to HSA induces alterations in the structure and function of this protein. However, competitive binding displayed by different ligands may result from allosteric effects, whereby binding of ligand A at a certain site causes a conformational change in the protein so that binding of ligand B at a different site is altered (Miles *et al.*, 1962).

#### Energy transfer between TPL and protein

The spectral studies suggested that HSA forms a complex with TPL. HSA has a single tryptophan residue (Trp-214). The distance  $r$  between Trp-214 in HSA and the bound TPL could be determined using fluorescence resonance energy transfer (FRET) (Jiaquin *et al.*, 2003). Generally, FRET occurs whenever the emission spectrum of a fluorophore

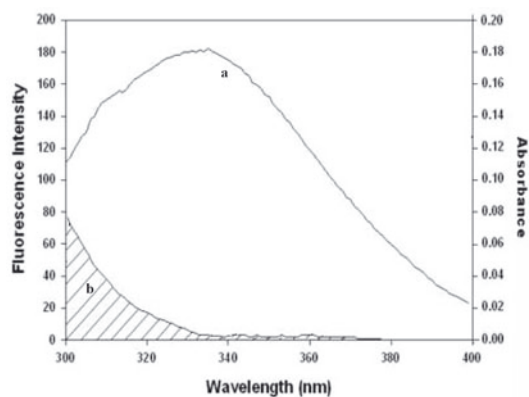


Figure 10. Förster resonance energy transfer (FRET). Overlap of fluorescence spectrum of HSA (a) and the absorbance spectrum of TPL (b) [ $c(\text{HSA})/c(\text{TPL}) = 1:1$ ].

(donor) overlaps the absorbance spectrum of another molecule (acceptor). The overlap of the UV absorbance spectrum of TPL with the fluorescence emission spectra of HSA is shown in Fig. 10. The distance between the donor and acceptor and extent of spectral overlaps determines the extent of energy transfer. The distance between the donor and acceptor can be calculated according to Förster's theory (Förster & Sinanoglu, 1996). The efficiency of energy transfer,  $E$ , is calculated using the equation:

$$E = 1 - \frac{F}{F_0} = \frac{R_0^6}{R_0^6 + r^6} \quad (10)$$

where  $F$  and  $F_0$  are the fluorescence intensities of HSA in the presence and absence of TPL,  $r$  is the distance between acceptor and donor, and  $R_0$  is the critical distance when the transfer efficiency is 50%.

$$R_0^6 = 8.8 \times 10^{-25} (k^2 \eta^{-4} \Phi J) \quad (11)$$

where  $k^2$  is the spatial orientation factor of the dipole,  $\eta$  the refractive index of the medium,  $\Phi$  the fluorescence quantum yield of the donor and  $J$  is the overlap integral of the fluorescence emission spectrum of the donor and the absorbance spectrum of the acceptor.  $J$  is given by equation:

$$J = \frac{\sum F(\lambda) \varepsilon(\lambda) \lambda^4 \Delta\lambda}{\sum F(\lambda) \Delta\lambda} \quad (12)$$

where  $F(\lambda)$  is the fluorescence intensity of the fluorescent donor at wavelength,  $\lambda$ , and  $\varepsilon(\lambda)$  is the molar absorption coefficient of the acceptor at wavelength,  $\lambda$ . In the present case,  $k^2 = 2/3$ ,  $N = 1.336$  and  $\Phi = 0.118$  for HSA (Epps *et al.*, 1999). From Eqns. (9) to (11), we were able to calculate that  $J = 2.3 \times 10^{-15} \text{ cm}^3 \text{ L mol}^{-1}$ ,  $R_0 = 1.92 \text{ nm}$ ,  $E = 0.24$  and  $r = 2.32 \text{ nm}$

for HSA. The donor-to-acceptor distance,  $r < 8 \text{ nm}$  (Valeur & Brochon, 1999), indicated that the energy transfer from HSA to TPL occurs with high possibility. Larger HSA-TPL distance ( $r$ ) to that of critical distance ( $R_0$ ), also reveals the presence of static type quenching mechanism (Valeur & Brochon, 1999; He *et al.*, 2005).

#### The effect of ions on the binding constant of TPL-protein

In plasma, there are some metal ions which can affect the reactions of drugs with serum albumins. The effects of common ions, *viz.*,  $\text{Cu}^{2+}$ ,  $\text{Fe}^{3+}$ ,  $\text{Ni}^{2+}$ ,  $\text{Zn}^{2+}$ ,  $\text{Mn}^{2+}$  and  $\text{Ca}^{2+}$  on the binding constants of the TPL-HSA system were investigated at 298 K by recording the fluorescence intensity in the range of 300–400 nm upon excitation at 280 nm. As evident from Table 5, the presence of metal ions increased the basic binding constants ( $K$ ) to ( $K'$ ), showing an increased persistence of TPL in the blood and so its effects, which may lead to the need for dose reduction of TPL to achieve the desired therapeutic effect (Li *et al.*, 2005; Pang *et al.*, 2005).  $K'/K$  signifies the fold increase in the binding constant.

#### CONCLUSION

TPL is a common intravenously administered barbiturate anesthetic and its interaction with serum albumin is of prime significance. The interaction was investigated by UV-visible, fluorescence, FT-IR and CD spectroscopic techniques. The UV-visible spectroscopy reveals a red-shift which is indicative of TPL binding with HSA. The fluorescence spectroscopy revealed a complex formation at 1:1 concentration of TPL and HSA at physiological pH. The interaction was linearly dependent on HSA concentration. The TPL binding was also found to be conformation-dependent and the highest association constant was observed for the F-isomer of HSA. The TPL-binding pockets were found to be located on domain-II of the protein. The static type of quenching is indicative of a complex formation between the protein and the drug molecule. Drug interactions will in most cases significantly affect the apparent distribution volume of the drugs and also affect the elimination rate and determine the therapeutic affectivity of drugs. At the plasma concentration of HSA the fraction of free drug was found to be 71% more for N isomer than F isomer. The binding is mediated mainly by hydrogen bonding and hydrophobic interaction. The perturbation of protein secondary structure on TPL binding is suggestive of anesthetic induced protein dysfunction.

## Acknowledgements

We are thankful to the central instrumentation facility of IBU. This work was supported by the CSIR sanction no. 37(1209)04 EMR II. The authors S.N.K. and B.I. acknowledge the fellowship from CSIR, India.

## REFERENCES

- Ahmad B, Parveen S, Khan RH (2006) Effect of albumin conformation on the binding of ciprofloxacin to human serum albumin: a novel approach directly assigning binding site. *Biomacromolecules* : 1350–1356.
- Aki H, Yamamoto M (1989) Thermodynamics of the binding of phenothiazines to human plasma, human serum albumin and alpha 1-acid glycoprotein: a calorimetric study. *J Pharm Pharmacol* **41**: 674–679.
- Borga O, Borga B (1997) Serum protein binding of nonsteroidal anti-inflammatory drugs: a comparative study. *J Pharmacokinetic Biopharm* **25**: 63–77.
- Chamouard JM, Barre J, Urien S, Houin G, Tillement JP (1985) Diclofenac binding to albumin and lipoproteins in human serum. *Biochem Pharmacol* **34**: 1695–1700.
- Chen YH, Yang JT (1971) A new approach to the calculation of secondary structures of globular proteins by optical rotatory dispersion and circular dichroism. *Biochem Biophys Res Commun* **44**: 1285–1291.
- Chmelik J, Kalous V (1982) Polarographic investigation of conformational changes of human serum albumin. *Bioelectrochem Bioenerg* **9**: 7–13.
- Cui F-L, Fan J, Li J-P, Hu Z (2004) Interactions between 1-benzoyl-4-p-chlorophenyl thiosemicarbazide and serum albumin: investigation by fluorescence spectroscopy. *Bioorg Med Chem* **12**: 151–157.
- Dugaiczky A, Law SW, Dennison OE (1982) Nucleotide sequence and the encoded amino acids of human serum albumin mRNA. *Proc Natl Acad Sci USA* **79**: 71–75.
- Epps DE, Raub TJ, Caiolfa V, Chiari A, Zamai M (1999) Determination of the affinity of drugs toward serum albumin by measurement of the quenching of the intrinsic tryptophan fluorescence of the protein. *J Pharm Pharmacol* **51**: 41–48.
- Förster T, Sinanoglu O, eds (1996) *Modern Quantum Chemistry*, p. 93. Academic Press, New York.
- Feng X-Z, Lin, Z, Yang L-J, Wang C, Bai C-L (1998) Investigation of the interaction between acridine orange and bovine serum albumin. *Talanta* **47**: 1223–1229.
- Gao H, Lei L, Liu J, Qin K, Chen X, Hu Z (2004) The study on the interaction between human serum albumin and a new reagent with antitumour activity by spectrophotometric methods. *J Photochem Photobiol Part A* **167**: 213–221.
- Gelamo EL, Silva CHTP, Imasato H, Tabak M (2002) Interaction of bovine (BSA) and human (HSA) serum albumins with ionic surfactants: spectroscopy and modeling. *Biochim Biophys Acta* **1594**: 84–99.
- Giraud O, Dehoux M, Rolland C, Mantz J, Malas V, Toueg ML, Desmonts JM, Aubier M (1998) Differential effects of halothane and thiopental on the lung inflammatory response after LPS-induced lung injury in the rat. *Anesthesiology* **89**: 34–38.
- He W, Li Y, Xue C, Hu Z, Chen X, Sheng F (2005) Effect of Chinese medicine alpinetin on the structure of human serum albumin. *Bioorg Med Chem* **13**: 1837–1845.
- Hu YJ, Liu Y, Wang JB, Xiao XH, Qu SS (2004) Study of the interaction between monoammonium glycyrrhizinate and bovine serum albumin. *J Pharm Biomed Anal* **36**: 915–919.
- Hu YJ, Liu Y, Shen XS, Fang XY, Qu SS (2005) Studies on the interaction between 1-hexylcarbamoyl-5-fluorouracil and bovine serum albumin. *J Mol Struct* **738**: 143–147.
- Jiaquin L, Jianniao T, Zhang J, Hu Z, Xingguo C (2003) Interaction of magnolol with bovine serum albumin: a fluorescence-quenching study. *Anal Bioanal Chem* **376**: 864–867.
- Khan MY (1986) Direct evidence for involvement of domain III in the N-F transition of bovine serum albumin. *Biochem J* **236**: 307–310.
- Khan SN, Islam B, Khan AU (2007) Probing midazolam interaction with human serum albumin and its effect on structural state of protein. *Int J Integ Biol* **2**: 102–112.
- Kragh-Hansen U (1981) Molecular aspects of ligand binding to serum albumin. *Pharmacol Rev* **33**: 17–53.
- Krier C, Wiedemann K, Polarz H (1984) Hazards of high dose barbiturate therapy in head-injury patients. *Acta Anaesthesiol Belg* **35**: 361–369.
- Li Y, He W, Liu J, Sheng F, Hu Z, Chen X (2005) Binding of the bioactive component jatrorrhizine to human serum albumin. *Biochim Biophys Acta* **1722**: 15–21.
- Lloyd JBF (1971) Synchronized excitation of fluorescence. emission spectra. *Nat Phys Sci* **231**: 64–65.
- Martin BK (1965) Potential effect of the plasma proteins on drug distribution. *Nature* **207**: 274–276.
- Miles JL, Morey E, Crain F, Gross S, San Julian J, Canady WJ (1962) Inhibition of  $\alpha$ -chymotrypsin by diethyl ether and certain alcohols: a new type of competitive inhibition. *J Biol Chem* **237**: 1319–1322.
- Miller JN (1979) Recent advances in molecular luminescence analysis. *Proc Anal Div Chem Soc* **16**: 203–208.
- Neault JF, Tajmir-Riahi HA (1998) Interaction of cisplatin with human serum albumin: Drug binding mode and protein secondary structure. *Biochem Biophys Acta* **1384**: 153–159.
- Pang YH, Yang LL, Shuang SM, Dong C, Thompson M (2005) Interaction of human serum albumin with bendroflumethiazide studied by fluorescence spectroscopy. *J Photochem Photobiol Part B* **80**: 139–144.
- Peters T Jr (1996) All about albumin: biochemistry, genetics and medical application. Academic Press, Inc, NY.
- Rahman MH, Maruyama T, Okada T, Yamasaki K, Otogiri M (1993) Study of interaction of carprofen and its enantiomers with human serum albumin-I. *Biochem Pharmacol* **46**: 1721–1731.
- Ross PD, Subramanian S (1981) Thermodynamics of protein association reactions. Forces contributing to stability. *Biochemistry* **20**: 3096–3102.
- Ryan CW, Vogelzang NJ, Vokes EE, Kindler HL, Undevia SD, Humerickhouse R, Andre AK, Wang Q, Carr RA, Ratain MJ (2004) Dose-ranging study of the safety and pharmacokinetics of atrasentan in patients with refractory malignancies. *Clin Cancer Res* **10**: 4406–4411.
- Schalen W, Messeter K, Nordstrom CH (1992) Complications and side effects during thiopentone therapy in patients with severe head injuries. *Acta Anaesthesiol Scand* **36**: 369–377.
- Seedher N, Singh B, Singh P (1999) Mode of interaction of metronidazole with bovine serum albumin. *Indian J Pharm Sci* **61**: 143–148.
- Sereikaite J, Bumelis VA (2006) Congo red interaction with  $\alpha$ -proteins. *Acta Biochim Polon* **53**: 87–92.
- Skarlosh (1974) Effect of thiopental sodium on the biligenic function of the liver. *Farmacol Toksikol* **37**: 701–702.

- Surewicz WK, Mantsch HH, Chapman D (1993) Determination of protein secondary structure by Fourier-transform infrared spectroscopy: a critical assessment. *Biochemistry* **32**: 389–394.
- Tian JN, Liu JQ, Zhang JY, Hu ZD, Chen XG (2003) Fluorescence studies on the interactions of barbaloin with bovine serum albumin. *Chem Pharm Bull* **51**: 579–582.
- Valeur B, Brochon JC (1999) *New Trends in Fluorescence Spectroscopy*. 6th edn, p. 25. Springer Press, Berlin.
- Ware WR (1962) Oxygen quenching of fluorescence in solution, an experimental study of the diffusion process. *J Phys Chem* **66**, 455–458.
- Wilting J, Vander Glesen WF, Janssen LH, Weideman MM, Otagiri M, Perrin JH (1980) The dependence of the binding of warfarin to human serum albumin on the hydrogen, calcium and chloride ion concentrations as studied by circular dichroism, fluorescence, and equilibrium dialysis. *J Biol Chem* **255**: 3032–3037.